Unequal Error Protection TCM Codes [1]

Dr. Jaehyeong Kim

Lucent Technologies

67 Whippany Road, Room 1A-256

Whippany, NJ 07981-0903, U.S.A.

(phone) 973 386 7883

(e-mail) kimj@lucent.com

Dr. Gregory J. Pottie

Associate professor

Dept. of Electrical Engineering

University of California, Los Angeles

405 Hilgard Ave.

Los Angeles, CA 90024, U.S.A.

(phone) 310 825 8150

(e-mail) pottie@icsl.ucla.edu

[1] This work is supported by David Sarnoff Research Center and state of California under terms of MICRO contract 93-075.

Abstract

We consider a family of unequal error protection(UEP) codes using multilevel codes and a four-way partition of one dimensional lattice. The non-regular set partitioning combined with non-uniform signal constellation yields codes with large minimum distance and small path multiplicity. However, this is not in itself sufficient for reliable coding gain estimation. New code search methods are introduced for better estimation of actual coding gain results. We present codes which permit resolution of phase ambiguities while providing gain comparable to the best previously published results.

Key words : *unequal error protection code.*

1. Introduction

In broadcast systems, the channels for each customer are different. With analog transmission, the result is a variable quality of reception, which depends roughly on the range from the transmitter. In digital systems, the design usually guarantees a uniformly good quality of service up to a given range, after which point the service rapidly deteriorates. For example, in digital HDTV, forward error correction coding will be used to increase the range of high quality service. However, it is possible to perform coding such that customers may receive a lower resolution signal even when the high definition part of the signal is lost, so that a quality of service comparable for example to NTSC can be obtained out past the range of ordinary analog transmission. Unequal error protection (UEP) codes give more protection to the low-rate important information, and thus are suitable for similar broadcast systems.

Cover [8] has considered the maximum achievable capacity over broadcast channels that may have differing capacities. Two forms of transmission (time sharing and superimposing) were considered, with superimposition shown to be better than time sharing in terms of channel capacity.

Time sharing allocates time slots to different rates of transmission. In time sharing for UEP, two or more coded modulation schemes provide different levels of error protection for different class data in different time slots. Generalized time sharing where a code of non-zero rate specifies the multiplexing rule has been proposed [1]. Additional important bits can be transmitted in this scheme.

In the superimposition technique, information for all the classes is sent at the same time. The low-rate data is recovered when the channel is not good enough to recover all the information. Uncoded non-uniform constellations where there are several clusters (or groups) of signal points and the inter-group distance is larger than the intra-group distance have been considered for a simple superimposing scheme [9]. Wei has proposed a UEP code which has 90^o rotational invariance [2] [14]. In his scheme, the rotationally invariant (RI) code is used only for important data because the phase rotation does not change the non-important data decoding results. However the non-important data coding gain is

not satisfactory. Calderbank and Seshadri have proposed various kinds of UEP codes for different ratios of important to less important data by using multilevel codes which can allocate the available redundancy in a rather flexible manner [1] [3] [4]. They have used a non-standard set partitioning as well as non-uniform signal constellations to reduce the path multiplicity. The coding gain reduction of non-important data due to non-standard set partitioning can be compensated by using additional coders.

We consider extensions of this work on superimposition of class 1 (important bits) and class 2 (less important bits) data. Ordinary TCM on QAM has an innate capability in this regard. Consider rate-1/2 TCM as an example. The squared minimum distance d^2_{min} of the 16-state rate-1/2 convolutional code is 7 and the d^2_{min} of the uncoded bits is 4. We can easily achieve two-level UEP by using the convolutional coder for class 1 data. However the standard set partitioning causes a large path multiplicity which reduces the class 1 coding gains significantly.

TCM based on PAM signalling results in convolutionally coded bits with larger d^2_{min} and much lower path multiplicity. However, this 1-D signalling scheme is not power efficient. We propose to compensate for this inefficiency by locating the signal points for less important data on another 1-D axis. In this case, a standard code search does not give us reliable information on d^2_{min} and corresponding path multiplicities because the code is not geometrically uniform. New code search methods will be introduced for better estimation of the actual coding gain. All the schemes we are considering have the same basic structure as mentioned above.

Our schemes can have 90^o rotational immunity by using a 180^o RI rate-1/2 convolutional code for class 1 data and then resolving the in-phase and quadrature-phase power. Like the Wei UEP code scheme, the coders for class 2 data do not have to be RI coders.

The paper is organized as follows. In section 2, we discuss coding gain calculations. The UEP code family based on set partitioning on one-dimensional lattices will be discussed in section 3, 4 and 5. Methods to design 90^o rotationally invariant codes are discussed in section 6. Some simulation results and concluding remarks are presented in section 7.

2. Coding Gain Calculations

Coding gain is a function of various factors including redundancy, constellation expansion, constellation power penalty, minimum distance and path multiplicity. The path multiplicity N_f is the number of nearest neighbors and the normalized path multiplicity N_f^* is N_f per 2 dimensions. $N_f^* = N_f/N$ when we use 2N dimensional signalling. Denote by E_N the penalty due to large path multiplicity. If N_f^* is less than 4 we have gains due to small path multiplicity, because N_f for uncoded QAM is 4. Using the rule of thumb that doubling N_f causes a 0.2 dB degradation at error probability 10^{-6} [13],

$$E_N = 0.2 \log_2(\frac{N_f^*}{4}). \tag{1}$$

Let P be the average power of the proposed scheme and let an uncoded M-QAM of average power P_{ref} be the reference scheme. Then the power penalty E_P can be obtained as

$$E_P = 10 \log \frac{P}{P_{ref}} \tag{2}$$

Let R be the bit rate per two dimensions. The rate loss ρ is defined as $R - \log_2 M$. Then the penalty due to rate loss E_R is 3.01ρ. The asymptotic coding gain G is obtained in equation (3).

$$G = 10 \log d_{min}^2 - E_P - E_R \tag{3}$$

Where d_{min} is the minimum distance. We now turn to the distance properties of TCM. Consider first the minimum distance property of binary convolutional codes. Let Ψ_B be a set of binary codewords, and Z^+ be the set of positive integers. Since convolutional codes are linear, for all $B_i, B_j \in \Psi_B$ there exist $B_k \in \Psi_B$ such that $B_i \oplus B_j = B_k$, where $\oplus$ is bitwise modulo 2 addition and $i, j, k \in Z^+$. Then,

$$d_H(B_i, B_j) = W_H(B_k) = d_H(B_0, B_k) \tag{4}$$

where d_H is the Hamming distance, W_H is the Hamming weight and B_0 is the all-zero codeword. Assume B_i is a reference codeword, d_{Hn} ($n \in Z^+$ and $d_{Hn} < d_{Hl}$, if $n < l$)

are the possible Hamming distances between B_i and other codewords, and $N_f(d_{Hn})$ is the number of codewords at distance d_{Hn} from the reference B_i. Ω_{Bi} is defined to be the set of elements $(d_{Hn}, N_f(d_{Hn}))$. From the equation (4), we see that $\Omega_{Bi} = \Omega_{B0}$ for all i such that $B_i \in \Psi_B$. Thus the convolutional code has the following property [12].

Property 1 The set of distances of the code sequences generated up to some stage in the tree, from the all zero sequence, is the same as the set of distances of the code sequences with respect to any other code sequence.

From *property 1* we can calculate the minimum distance assuming that the all zero sequence is the input to the encoder. This zero-path reference code search (ZRCS) considerably simplifies the search for codes with large d_{min}. Calderbank and Sloane [6], Benedetto *et al.*, [7] and Forney [5] investigated the conditions sufficient to ensure that a coset code [13] is distance-invariant, so that d_{min} and path multiplicity of the code do not depend on the transmitted code sequence. Apart for the boundary region of the constellation, ordinary TCM based on standard set partitioning of regular lattice satisfies *property 1*, and we can use ZRCS for good estimates. Otherwise, the code search is quite complex and we need to find a new approach. For that purpose, we also derive the sufficient conditions which allow ZRCS in TCM code search.

Let Φ be the set of cosets such that $\Phi = \{\xi_0, \xi_1, ..., \xi_{M-1}\}$, where M is the number of cosets. Let $d^2(\xi_i, \xi_j)$ be the squared Euclidean distance between cosets ξ_i and ξ_j and the *kissing number* $\eta(\xi_i, \xi_j)$ be the number of signal points in coset ξ_j which are at the distance $d(\xi_i, \xi_j)$ to coset ξ_i. Let Ψ_C be a set of codewords in TCM. The codeword $C_i \in \Psi_C$ is a sequence of cosets and is expressed as $C_i = (c_{i1}, c_{i2}, ...)$, where $c_{it} \in \Phi,\ t \in Z^+$. Ψ_C is a homomorphic set of Ψ_B and there is a one to one mapping $\tau(.)$ between the codewords $C_i \in \Psi_C$ and $B_i \in \Psi_B$, such that $\tau(C_i) = B_i$ and $\tau^{-1}(B_i) = C_i$. Every $m(= \log_2 M)$ bits of B_i are grouped to be a binary label of coset sequences in C_i. The operation $\diamond$ in the set Ψ_C is defined as follows.

$$C_i \diamond C_j \equiv \tau^{-1}(\tau(C_i) \oplus \tau(C_j))$$

The distance between codewords can be obtained as follows.

$$d^2(C_i, C_j) = \sum_{t=1}^{T} d^2(c_{it}, c_{jt}) \tag{5}$$

where T is larger than the largest codeword.

Unlike the binary codewords in convolutional codes, codewords in TCM may have multiple paths when each coset has more than one member. Define $\mu(C_i, C_j)$ to be the number of paths of C_j at the distance $d^2(C_i, C_j)$ to C_i. Then,

$$\mu(C_i, C_j) = \prod_{t=1}^{t=T} \eta(c_{it}, c_{jt}). \tag{6}$$

Assume C_i is a reference codeword, and d_n^2 ($n \in Z^+$ and $d_n^2 < d_l^2$, if $n < l$) is the possible squared Euclidean distance between C_i and any other codeword and $N_f(d_n^2)$ is the number of codeword paths at distance d_n^2 from the reference C_i. $N_f(d_n^2)$ can be obtained as follows.

$$N_f(d_n^2) = \sum_{d^2(C_i, C_j) = d_n^2} \mu(C_i, C_j) \tag{7}$$

Ω_{Ci} is defined as the set of element $(d_n^2, N_f(d_n^2))$ when $C_i \in \Psi_C$ is a reference codeword. If Ω_{Ci} is Ω_{C0} for all $C_i \in \Psi_C$, we can use ZRCS for the code search. The sufficient conditions for ZRCS in TCM can be derived from equations (5,6,7), and described as follows.

For all $\xi_i, \xi_j, \xi_k, \xi_0 \in \Phi$ such that $\xi_i \diamond \xi_j = \xi_k$, where ξ_0 is a coset with all-zero binary notation, if the following conditions are satisfied, we can use ZRCS.

condition 1 $d^2(\xi_i, \xi_j) = d^2(\xi_0, \xi_k)$.

condition 2 $\eta(\xi_i, \xi_j) = \eta(\xi_0, \xi_k)$.

If there is more than one member per coset, the values of $d^2(\xi_i, \xi_j)$ and $\eta(\xi_i, \xi_j)$ might depend on a specific choice of members in each coset. For example, the kissing numbers of cosets at the boundary and inside the constellation could be different. In this case, the two conditions are quite difficult to satisfy. Standard four-way set partitioning on uniform 64-QAM constellation is illustrated in Figure 1, where *condition 1* is satisfied for all the

points but *condition 2* is not satisfied for some points at the boundary of the constellation. However, most of them satisfy both conditions and we can use ZRCS without much error.

For non-standard partitioning, we may instead use a statistical modification of ZRCS (S-ZRCS), where the all-zero path is still used as a reference but the squared distances and kissing numbers of cosets are varied depending on the transmitted codeword or in a random manner. The S-ZRCS algorithm is briefly described as follows. Codes are randomly generated and we obtain the corresponding sequences of cosets. Suppose that $\xi_i \diamond \xi_j = \xi_k$, $d^2(\xi_i, \xi_j) \neq d^2(\xi_0, \xi_k)$ and $\eta(\xi_i, \xi_j) \neq \eta(\xi_0, \xi_k)$. The metric $M_e(\xi_k)$ and kissing number $K(\xi_k)$ of the branch labeled ξ_k are $d^2(\xi_0, \xi_k)$ and $\eta(\xi_0, \xi_k)$, respectively if ξ_0 is transmitted, or they are $d^2(\xi_i, \xi_j)$ and $\eta(\xi_i, \xi_j)$ if ξ_i is transmitted. Then we obtain the possible distances and corresponding path multiplicities. In general, $d^2(\xi_i, \xi_j)$ and $\eta(\xi_i, \xi_j)$ may have different values for different signal points in coset ξ_i. Thus we have multiple reference paths, even though there is a single reference sequence of cosets (all zero path) in the code search. We choose a signal points within cosets in an equiprobable manner and assign the corresponding values to the distance metric and kissing number. After many trials, we obtain the possible distances and corresponding average path multiplicities. According to simulations, several hundred trials gives good results for a 16-state trellis.

From the previously described code search, we obtain the possible squared Euclidean distances d_n^2 ($n \in Z^+$ and $d_n^2 < d_l^2$ if $n < l$) and corresponding average path multiplicities $N_f^*(d_n^2)$ per 2-D. Then, the component coding gain α_n, $n \in Z^+$, is defined as

$$\alpha_n = 10 \log d_n^2 - 0.2 \log_2 \left(\frac{N_f^*(d_n^2)}{4} \right) \tag{8}$$

A code search finds the generator sequence which maximizes the value $\min \alpha_i$ We define the actual coding gain G_a as

$$G_a = \max \left(\min_{n \in Z^+} \alpha_n \right) - E_P - E_R \tag{9}$$

A family of multilevel UEP codes using set partitioning on one-dimensional lattices will be considered. Uncoded 16-QAM is considered as a reference scheme in coding gain calculations and simulations.

3. Scheme I

We use 16-QAM and 64-QAM in both 2 and 4 dimensional signal constellations. The coset partitioning and signal constellations are shown in Figure 2, where we can change the in-phase distance between signal points by changing the value of k.

3.1. Two dimensional signalling scheme

Code structures using 16-QAM and 64-QAM are shown in Figure 3. There are two schemes (scheme I-A and scheme I-B) for 16-QAM and 64-QAM. The code structure of scheme I-A is illustrated in Figure 3 (a) and (b). Scheme I-A uses 16-state rate-1/2 TCM for class 1 data, where the signal looks like 4-PAM or 8-PAM with 4 cosets (A, B, C and D). The code search follows the procedure of the previous section.

In both cases, the squared minimum distance (d_1^2) of code C_1 is 11. The code search results using S-ZRCS are given in Table 1. The class 2 data are protected by 8 dimensional rate-3/4 punctured TCM, where one output bit of a rate-3/4 convolutional code is assigned for each two-dimensional signal. The d_{min}^2 of code C_2 is $4k^2$.

For example, we calculate the coding gains when k^2 is 1. Let Γ and Γ_a are asymptotic coding gain and actual coding gain for class 1 data, respectively. γ is asymptotic coding gain for class 2 data. Let the uncoded 16-QAM be the reference scheme for calculation of E_P and E_R. In scheme I-A on 16-QAM, E_P = 0 and E_R is 3.75 dB ($R = 2.75$ and ρ = 1.25). Thus, from equations (8,9),

$$\begin{aligned} \min_{i \in Z^+} \alpha_i &= \alpha_2 = 11.02(\text{dB}). \\ \Gamma_a &= 11.02 - 3.75 = 7.27(\text{dB}). \\ \gamma &= 10\log_{10} 4 - 3.75 = 2.27(\text{dB}). \end{aligned}$$

For 64-QAM, E_P = 6.23 dB and E_R is -2.25 dB ($R = 4.75$ and ρ = -0.75).

$$\begin{aligned} \min_{i \in Z^+} \alpha_i &= \alpha_1 = 10.83(\text{dB}). \\ \Gamma_a &= 10.83 - 6.23 + 2.25 = 6.85(\text{dB}). \\ \gamma &= 10\log_{10} 4 - 6.23 + 2.25 = 2.04(\text{dB}). \end{aligned}$$

Consider another scheme (scheme I-B) which shows better performance. The code structure is illustrated in Figure 3 (c) and (d). The difference here is that for protecting the class 2 data, we use a 16-state rate-1/2 convolutional code which assigns one output bit per two-dimensional signal and also a single parity check code to improve the intra-coset distance. In this case, we assign 1 bit for class 1 data and 1.5 bits for class 2 data for 16-QAM or 2 bits and 2.5 bits for each classes for 64-QAM. The minimum distance of class 1 data is not changed. Since the d^2_{min} of parity check code is $8k^2$, the minimum distance of class 2 data, $d^2_{min}(C_2)$, is $\min(7k^2, 8k^2)$. The value $7k^2$ comes from the fact that the minimum distance of the 16-state rate-1/2 convolutional code is 7.

For example, we calculate the coding gains when k^2 is 0.7. Let L be the block length of the parity check code. For 16-QAM, $E_R = 4.5 + 3/L$ dB (ρ = 1.5 + $1/L$), and E_P = -0.71 dB. For 64-QAM, $E_R = -1.5 + 3/L$ dB (ρ = -0.5 + $1/L$), and E_P = 5.53 dB. Thus, Γ_a is $7.23 - 3/L$ dB and γ is $3.11 - 3/L$ dB for 16-QAM. Γ_a is $6.5 - 3/L$ dB and γ is $2.87 - 3/L$ dB for 64-QAM. We may have higher coding gains for larger L. However, L can not be arbitrary increased. Increased path multiplicity due to large L starts to degrade the performance of class 2 code. We have found through simulation that $L = 20$ is good for all the cases presented in this paper. The degradation by using $L = 30$ is still less than 0.1 dB. Adding a single parity check code on the class 2 data gives us more gain.

In both schemes, we can trade-off the coding gains of the two classes by changing the value of k, i.e. a large value of k gives more gain for class 2 data while increasing the power penalty and thus reducing class 1 coding gain. From now on, we use scheme I-B for class 2 data protection.

3.2. Four dimensional signalling scheme

Four dimensional set partitioning can increase d^2_{min} of class 1 data. The 4-D coset labels are given in Table 2, and the 4-D metric structures of 16-QAM and 64-QAM are illustrated in Figure 4. When we use 16-QAM, only the signal points in the dashed rectangle can be considered. For 64-QAM, the right upper triangle part and the left lower triangle parts have the same metric structure. So we obtain the metric values for the 16 signal points

using the upper triangle. The code search results are in Table 3. The code structure is shown in Figure 5.

Consider 16-QAM. The d^2_{min} for class 1 data is increased from 11 to 14 but the path multiplicity is also increased by using the 4-D set partitioning. From the code search result,

$$\min_{i \in Z^+} \alpha_i = \alpha_1 = 11.26\text{(dB)}.$$

When k^2 = 0.7, Γ_a is $7.47 - 4.5/L$ dB, and γ is $3.11 - 4.5/L$. For 64-QAM, $E_R = -1.5 + 4.5/L$ ($\rho = -0.5 + 1.5/L$), and

$$\min_{i \in Z^+} \alpha_i = \alpha_1 = 10.92\text{(dB)}$$

Then, Γ_a is $6.89 - 4.5/L$ dB and γ is $2.87 - 4.5/L$. By using the the 4-D lattice, we can increase the d^2_{min} of the class 1 code. However, the increased path multiplicity reduces some part of gain obtained by increased d^2_{min}.

4. Scheme II

Using a non-uniform signal constellation may increase d^2_{min} in TCM [10]. The code structure of scheme II is the same as scheme I apart for those non-uniform signal constellations, as illustrated in Figure 6. Δ is another variable we use for the trade-off of class 1 and class 2 coding gains. Large Δ gives more gain for class 1 data. For example, we set $\Delta = 2.0$ and $k^2 = 1.5$. In 16-QAM signalling, d^2_{min} is increased from 11 to 26. $\min \alpha_i = \alpha_1 = 14.43$ (dB) (d^2_1 is 26 and $N_f(26)$ is 1.5). We pay a power penalty when Δ and k^2 are larger than 1(E_P = 2.43 dB). Then Γ_a is $7.5 - 3/L$ dB and γ is $3.28 - 3/L$ dB. For 64-QAM, E_P = 8.89 dB, $E_R = -1.5 + 3/L$ dB, and $\min \alpha_i = \alpha_1 = 14.15$ (dB) ($N_f(26)$ is 3.94). Then, Γ_a is $6.76 - 3/L$ dB and γ is $2.82 - 3/L$ dB. We have some gains from using non-uniform signal constellations in 16-QAM signalling by increasing d^2_{min} without increasing N_f.

We have also considered 4-D set-partitioning in this scheme. In this case, d^2_{min} is increased from 26 to 29. The coding gains are obtained as follows ($k^2 = 1.5$, Δ = 2.0). In 16-QAM, $\min \alpha_i = \alpha_1 = 14.62$ (dB) ($N^*_f(29)$ is 4.0) and $\Gamma_a = 7.69 - 4.5/L$ dB. In

64-QAM, $\min \alpha_i = \alpha_1 = 14.39$ (dB) ($N_f^*(29)$ is 9.02) and $\Gamma_a = 7.0 - 4.5/L$ dB. We have some gains over the 2-D scheme. However, for 64-QAM, the constellation expands too much in the Q-phase axis, causing a major power penalty.

5. Scheme III

In the previous schemes, the coding gains for 64-QAM are not as good as for 16-QAM. Here we trade a lower rate for important data against coding gains. The signal constellation and coset partitioning is shown in Figure 7. The code structure for 2-D signalling is shown in Figure 8 (a), where $d^2_{min} = 26$ and $\min \alpha_i = \alpha_1 = 13.97$ (dB) ($N_f(26)$ is 7.42). Unlike the previous schemes, the coding for class 2 data is not only a function of k^2 but also confined by the minimum distance of the parity check code, i.e. $d^2_{min} = \min(8, 7k^2)$. Thus the asymptotic coding gain of class 2 data is maximum when $k^2 = 8/7$. If we set Δ as 2.0, $E_P = 7.32$ dB and $E_R = -1.5 + 3/L$ dB. Then, Γ_a is $8.15 - 3/L$ dB and γ is $3.21 - 3/L$ dB. This code structure gives good coding gains to the two data classes with reasonable complexity (we use a 16-state rate-1/2 convolutional code for each class and a single parity check code for class 2 data protection). Furthermore, we can trade-off the two coding gains by changing the value of Δ.

We can further increase d^2_{min} for the class 1 code by using a 4-D set partitioning. The code structure for 4-D signalling is illustrated in Figure 8 (b). The code search result shows that $d^2_{min} = 29$ and $\min \alpha_i = \alpha_5 = 14.04$ (dB) ($N_f^*(34)$ is 330.71) and Γ_a is $8.22 - 4.5/L$ dB. Unlike the previous schemes, using 4-D signalling does not give us additional coding gain because of the big path multiplicity at the squared distance 34.

The actual coding gain of class 2 data is less than γ because of path multiplicity. When we let $k^2 = 8/7$, a large N_f for the rate-1/2 convolutional code for class 2 data contributes to the total N_f, which causes a large coding gain degradation. In a real situation, we may use a little bit larger value of k^2 to reduce the path multiplicity of the class 2 coder. Using the value of k^2 slightly larger than 8/7 can reduce N_f and increase the coding gain of class 2 data with the cost of a power penalty. For example, setting k^2 = 1.32, then there is an additional power penalty of 0.29 dB and Γ_a is $7.86 - 3/L$ dB in the 2-D scheme and

$7.93 - 4.5/L$ dB in the 4-D scheme. γ is $2.92 - 3/L$ dB for 2-D and $2.92 - 4.5/L$ dB for 4-D. Even though the asymptotic coding gain is reduced by 0.29 dB, the actual coding gain of class 2 data is increased by reducing N_f.

6. Rotationally Invariant UEP.

For the previously described codes to be 180^o rotationally invariant (RI), only the class 1 data protection code needs to be 180^o RI by assigning bit labels for class 2 data in a 180^o symmetric manner such that a 180^o phase rotation does not change the decoding results of the class 2 data. The bit labels for class 2 data with and without 180^o phase rotation are illustrated in Figure 9.

Now, consider having 180^o RI class 1 coders. In 2-D codes, flipping the output bits of the rate-1/2 convolutional code causes 180^o rotation of the cosets by assigning two bit labels 00, 01, 10, 11 to cosets A, B, C, D, respectively. Thus using 180^o RI rate-1/2 convolutional codes for class 1 data protection makes both classes of the UEP code 180^o rotationally invariant. This can be applied to 4-D codes. In Table 2, a bit flip of the output label corresponds to 180^o rotation of 4-D types and thus a bit flip of parity bits. For example, consider a 4-D type signal (A, A) which is 180^o rotated: we decode (D, D). Then the output label is bit flipped from 00 to 11 and the parity bit is flipped from 0 to 1. In this case, we need one more 180^o differential coder for the parity bits. The class 2 code structure is the same as for two dimensions. The structures of the 180^o RI class 1 codes are illustrated in Figure 10.

We can resolve 90^o phase ambiguities by using the fact that the in-phase average power P_I and the quadrature-phase average power P_Q are different. At the receiver, we measure the average power of the I and Q-phase directions and decide the polarity of the signal constellation. The remaining 180^o phase ambiguity can be resolved by using the previously described 180^o RI codes. The code search results for the 180^o RI codes are in Table 4. Fortunately, in all the schemes but II-B and III-B, the best generators have a 180^o RI structure. Thus we do not have to pay more to make these codes rotationally invariant. Coding gain calculations are summarized in Table 5.

7. Simulation Results and Conclusion

The simulation results for scheme III codes are in Figure 11. In this simulation, we fix the value of k^2 to 1.32 to reduce the path multiplicity of the class 2 code. Scheme III-B shows about 7 dB gain for class 1 data and about 2 dB gain for class 2 data at a 10^{-6} bit error rate. This scheme pays about 0.3 dB to have a 90^o RI structure. Scheme III-A having an RI structure shows about 0.4 dB less gain than scheme III-B without rotational invariance. However, scheme III-A could be the best choice if we want to have an RI code with less complexity.

The rotationally invariant UEP scheme proposed by Wei [2] provides good protection for the important bits, however the less important bits may even be less reliable than in uncoded transmission. Calderbank and Seshadri [1] suggested two approaches (generalized time sharing and superimposing) for UEP code design and provided greater protection for the less important bits than the Wei codes. Based on the simulation results (25% important bits) in their paper, they have achieved about 6.5 dB gain for the important bits and about 1.5 dB gain for the less important bits at a 10^{-6} bit error rate when they use time sharing. However, when they use a superimposing scheme, the less important bits were not protected.

We have considered a family of multilevel UEP codes based on superimposition for the additive white Gaussian channel. Four way partitioning in a one-dimensional lattice combined with a non-uniform signal constellation provides good coding gains for both data classes with reasonable complexity (at most, we use a 16-state rate-1/2 convolutional code and a single parity check code for each class of data protection). Furthermore, we can easily make 90^o rotationally invariant codes by using 180^o rotationally invariant rate-1/2 convolutional code and resolving in-phase and quadrature-phase power.

References

[1] A.R. Calderbank and N. Seshadri, "Multilevel codes for unequal error protection," *IEEE Trans. Inform. Theory,* vol. IT-39, no. 4, pp. 1234-1248, July. 1993.

[2] L.F. Wei, "Coded modulation with unequal error protection," *IEEE Trans. on Communications*, vol. 41, no.10, pp. 1439-1449, October 1993.

[3] A.R. Calderbank, "Multilevel codes and multistage decoding," *IEEE Trans. on Communications*, vol. 37, no. 3, pp. 222-229, March 1989.

[4] G.J. Pottie and D.P. Taylor, "Multilevel codes based on partitioning," *IEEE Trans. Inform. Theory,* vol. IT-35, no. 1, pp. 87-98, January 1989.

[5] G.D. Forney, Jr., "Geometrically uniform codes," *IEEE Trans. Inform. Theory,* vol. 37, no. 5, pp. 1241-1260, September 1991.

[6] A.R. Calderbank and N.A. Sloane, "New trellis codes based on lattices and cosets," *IEEE Trans. Inform. Theory,* vol. IT-33, no. 2, pp. 177-195, March 1987.

[7] S. Benedetto, M.A. Marsan, G. Albertengo and E. Giachin, "Combined coding and modulation : theory and applications," *IEEE Trans. Inform. Theory,* vol. IT-34, pp. 223-236, March 1988.

[8] T.M. Cover, "Broadcast channels," *IEEE Trans. Inform. Theory,* vol. IT-18, no. 1, pp. 2-14, January 1972.

[9] C.-E. W. Sundberg, W.C. Wong and R.S. Steele, "Logarithmic PCM weighted QAM transmission over Gaussian and Rayleigh fading channels," *IEEE Proc., pt. F,* vol. 134, no. 6, pp. 557-570, October 1987.

[10] D. Divsalar, M.K. Simon and J.H.Yuen, "Trellis coding with asymmetric modulations," *IEEE Trans. on Communications,* vol. 35, no. 2, February 1987.

[11] E. Biglieri, D. Divsalar, P.J. McLane and M.K. Simon, *Introduction to Trellis-Coded Modulation with Applications* Macmillan Publishing Company, 1991.

[12] J.G. Proakis *Digital Communications* McGraw-Hill Book Company, 1989.

[13] G.D. Forney Jr., "Coset codes Part I: Introduction and geometrical classification," *IEEE Trans. Inform. Theory,* vol IT-34, pp. 1123-1151, Sep. 1988.

[14] L.F. Wei, "Trellis-Coded Modulation with Multidimensional Constellations," *IEEE Trans. Inform. Theory,* vol IT-33, pp. 483-501, July 1987.

[15] G. Ungerboeck, "Channel coding with multilevel/phase signals," *IEEE Trans. Inform. Theory,* vol. IT-28, pp.55-67, Jan. 1982.

Figure 1: Four way partitioning in uniform 64-QAM constellation illustrating the two conditions for ZRCS.

Figure 2: Signal constellation for scheme I. (a) 16-QAM. (b) 64-QAM.

Figure 3: Code structures of scheme I using two dimensional signalling (code C1 is for class 1 data, and code C2 block is for class 2 data). (a) Scheme I-A on 16-QAM. (b) Scheme I-A on 64-QAM. (c) Scheme I-B on 16-QAM. (d) Scheme I-B on 64-QAM.

Figure 4: Four dimensional metric structure of scheme I-C.

Figure 5: Code structures of scheme I using four-dimensional signalling (code C1 block is for class 1 data and code C2 block is for class 2 data). (a) Scheme I-C on 16-QAM. (b) Scheme I-C on 64-QAM.

Figure 6: Non-uniform signal constellation for scheme II. (a) 16-QAM. (b) 64-QAM.

Figure 7: Signal constellation for scheme III. (a) 64-QAM constellation. (b) signal points for class 2 data (the points in the rectangle have the same parity bits).

Figure 8: Code structures of scheme III (code C1 block is for class 1 data and code C2 block is for class 2 data). (a) Scheme III-A(2-D signalling). (b) Scheme III-B(4-D signalling).

Figure 9: Signal constellation for 180^o RI scheme III. (a) Class 2 data bit allocation for 180^o RI code. (b) Received signal after 180^o phase error.

Figure 10: Structures of 180^o RI class 1 data protection code in scheme III. (a) 2-D signalling. (b) 4-D signalling.

Figure 11: Simulation of scheme III in 4-D signalling(k^2 is 1.32) and 180^o RI 2-D and 4-D signalling. Block length L of parity check code is 20. (a) Uncoded 16-QAM. (b) Class 2 data protection code. (c) class 1 code (scheme III-A : 90^o RIC on 2-D signalling). (d) class 1 code (scheme III-B : 90^o RIC on 4-D signalling). (e) class 1 code (scheme III-B : non-RIC on 4-D signalling).

Table 1: Code search results using S-ZRCS in scheme I-A and I-B.

Signal size	Average path multiplicity				
	$N_f(11)$	$N_f(12)$	$N_f(13)$	$N_f(14)$	$N_f(15)$
16-QAM	0.13	0.50	1.82	2.03	2.78
64-QAM	0.95	2.54	7.15	9.29	9.43

Table 2: Four dimensional set partitioning.

4-D sub-lattice	*4-D types*	
	parity bit 0	parity bit 1
0 (00)	(AA)	(CC)
1 (01)	(BD)	(DB)
2 (10)	(AC)	(CA)
3 (11)	(BB)	(DD)

Table 3: Code search results using S-ZRCS in scheme I-C.

Signal size	Average path multiplicity				
	$N_f^*(14)$	$N_f^*(16)$	$N_f^*(18)$	$N_f^*(20)$	$N_f^*(22)$
16-QAM	7.92	16.34	21.98	37.12	54.98
64-QAM	26.44	80.0	152.34	288.81	452.53

Table 4: Code search results of 16-state convolutional codes for class 1 data protection in scheme I, II and III (180^o RI and non-RI codes).

Scheme	best code		180^o RI-code	
	Generators(octal)	d^2_{min}	Generators(octal)	d^2_{min}
scheme I-A,B(2-D)	23,8	11	23,8	11
scheme I-C(4-D)	23,8	14	23,8	14
scheme II-A(2-D)	23,8	26	23,8	26
scheme II-B(4-D)	34,2	29	25,13	26
scheme III-A(2-D)	23,8	26	23,8	26
scheme III-B(4-D)	34,2	29	25,13	26

Table 5: Coding gains for the proposed UEP code family (L is the parity check code length).

Scheme	Signal Constellation		Class 1 Coding Gain (dB)	Class 2 Coding Gain (dB)
I-A (2-D) $k^2 = 1.0$	16-QAM 36.36 % class 1 data rate = 2.75	RI code	$\Gamma = 6.65$ $\Gamma_a = 7.27$	$\gamma = 2.27$
	64-QAM 42.11 % class 1 data rate = 4.75	RI code	$\Gamma = 6.43$ $\Gamma_a = 6.85$	$\gamma = 2.04$
I-B (2-D) $k^2 = 0.7$	16-QAM 40.0 % class 1 data rate = 2.5 - 1/L	RI code	$\Gamma = 6.62 - 3/L$ $\Gamma_a = 7.23 - 3/L$	$\gamma = 3.11 - 3/L$
	64-QAM 44.44 % class 1 data rate = 4.5 - 1/L	RI code	$\Gamma = 6.38 - 3/L$ $\Gamma_a = 6.50 - 3/L$	$\gamma = 2.87 - 3/L$
I-C (4-D) $k^2 = 0.7$	16-QAM 40.0 % class 1 data rate = 2.5 - 1.5/L	RI code	$\Gamma = 7.67 - 4.5/L$ $\Gamma_a = 7.47 - 4.5/L$	$\gamma = 3.11 - 4.5/L$
	64-QAM 44.44 % class 1 data rate = 4.5 - 1.5/L	RI code	$\Gamma = 7.43 - 4.5/L$ $\Gamma_a = 6.89 - 4.5/L$	$\gamma = 2.87 - 4.5/L$
II-A (2-D) $k^2 = 1.5$ $\Delta = 2.0$	16-QAM 40.0 % class 1 data rate = 2.5 - 1/L	RI code	$\Gamma = 7.22 - 3/L$ $\Gamma_a = 7.50 - 3/L$	$\gamma = 3.28 - 3/L$
	64-QAM 44.44 % class 1 data rate = 4.5 - 1/L	RI code	$\Gamma = 6.76 - 3/L$ $\Gamma_a = 6.76 - 3/L$	$\gamma = 2.82 - 3/L$
II-B (4-D) $k^2 = 1.5$ $\Delta = 2.0$	16-QAM 40.0 % class 1 data rate = 2.5 - 1.5/L	non-RI Code	$\Gamma = 7.69 - 4.5/L$ $\Gamma_a = 7.69 - 4.5/L$	$\gamma = 3.28 - 3/L$
	64-QAM 44.44 % class 1 data rate = 4.5 -1.5/L	non-RI Code	$\Gamma = 7.23 - 4.5/L$ $\Gamma_a = 7.00 - 4.5/L$	$\gamma = 3.05 - 4.5/L$
III-A (2-D) $k^2 = 1.14$ $\Delta = 2.0$	64-QAM 22.22 % class 1 data rate = 4.5 - 1/L	RI code	$\Gamma = 8.33 - 3/L$ $\Gamma_a = 8.15 - 3/L$	$\gamma = 3.21 - 3/L$
III-B (4-D) $k^2 = 1.14$ $\Delta = 2.0$	64-QAM 22.22 % class 1 data rate = 4.5 - 1.5/L	non-RI Code	$\Gamma = 8.80 - 4.5/L$ $\Gamma_a = 8.22 - 4.5/L$	$\gamma = 3.21 - 4.5/L$
		RI code	$\Gamma = 8.33 - 4.5/L$ $\Gamma_a = 7.99 - 4.5/L$	$\gamma = 3.21 - 4.5/L$

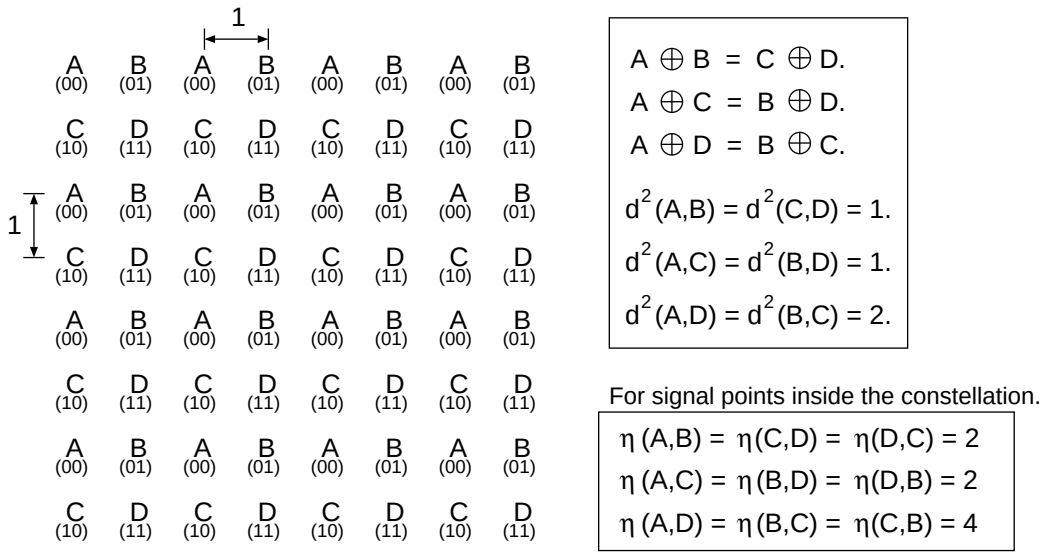

Figure 1: Four way partitioning in uniform 64-QAM constellation illustrating the two conditions for ZRCS.

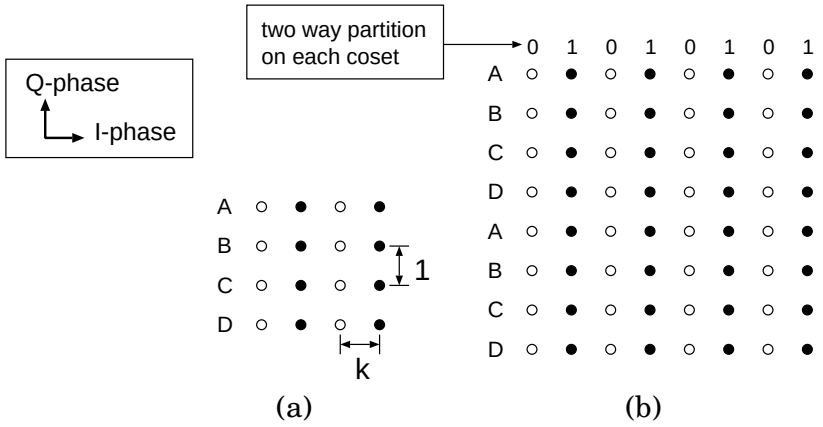

Figure 2: Signal constellation for scheme I. (a) 16-QAM. (b) 64-QAM.

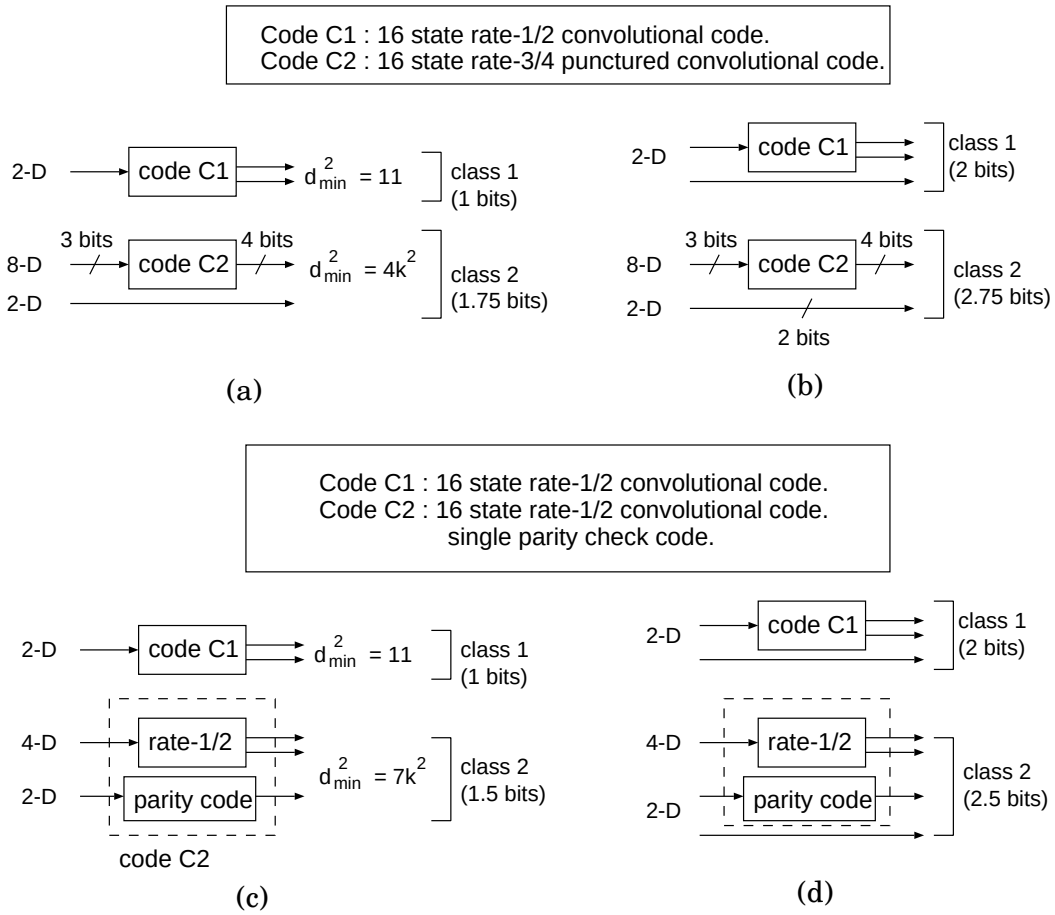

Figure 3: Code structures of scheme I using two dimensional signalling (code C1 is for class 1 data, and code C2 block is for class 2 data). (a) Scheme I-A on 16-QAM. (b) Scheme I-A on 64-QAM. (c) Scheme I-B on 16-QAM. (d) Scheme I-B on 64-QAM.

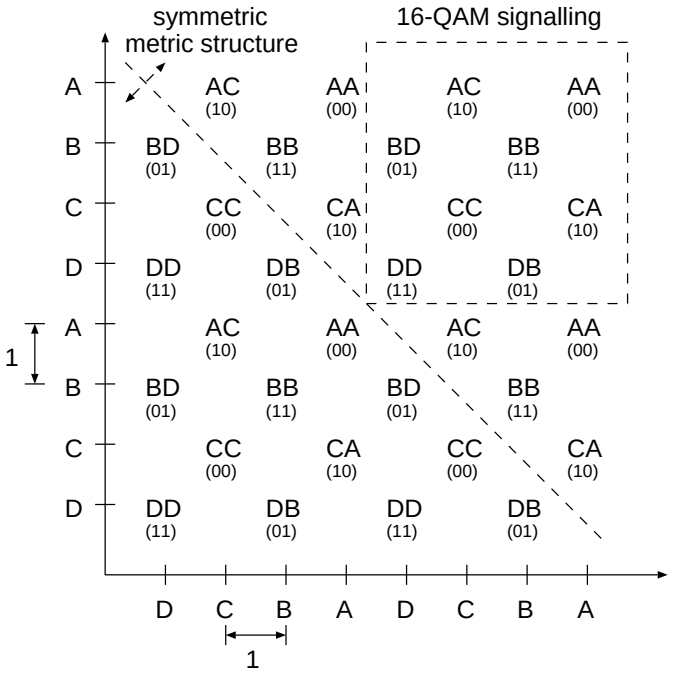

Figure 4: Four dimensional metric structure of scheme I-C.

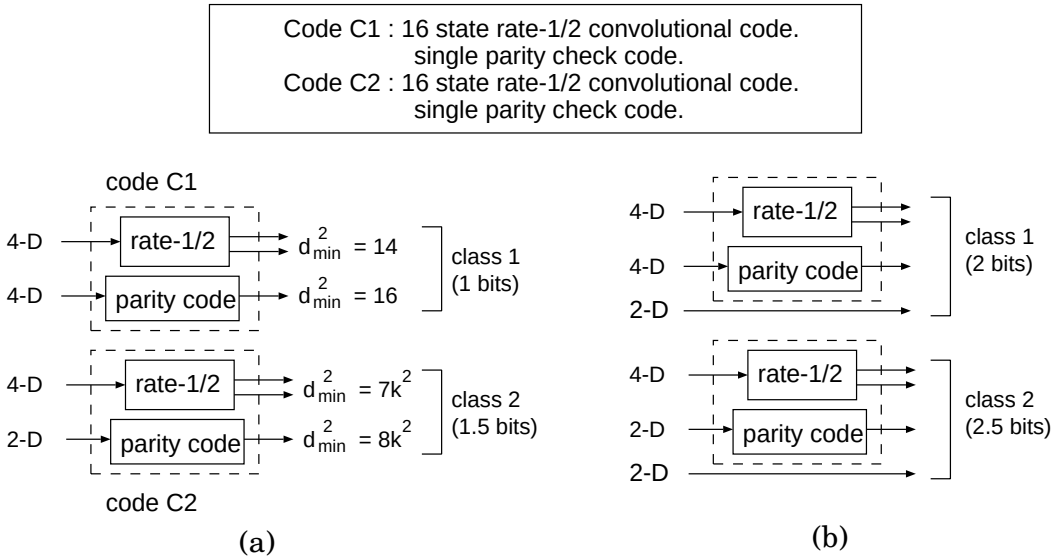

Figure 5: Code structures of scheme I using four-dimensional signalling (code C1 block is for class 1 data and code C2 block is for class 2 data). (a) Scheme I-C on 16-QAM. (b) Scheme I-C on 64-QAM.

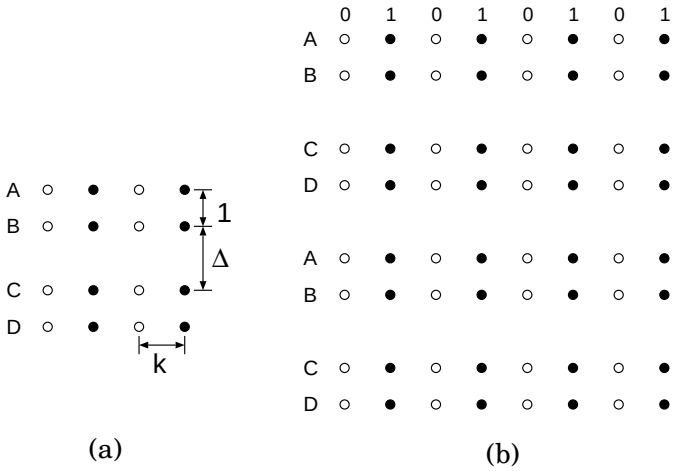

Figure 6: Non-uniform signal constellation for scheme II. (a) 16-QAM. (b) 64-QAM.

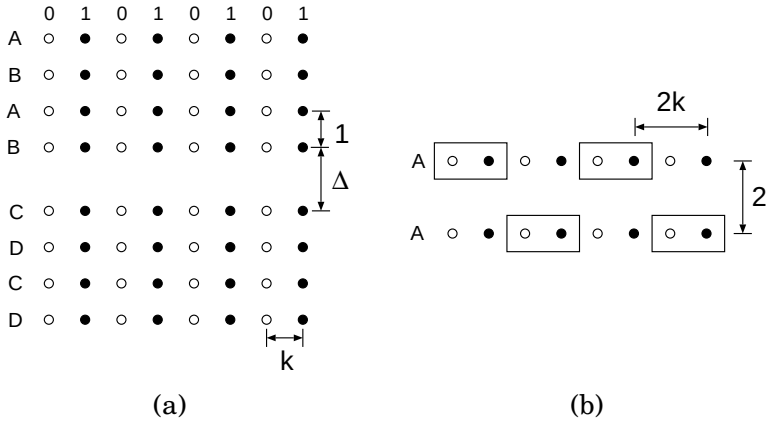

Figure 7: Signal constellation for scheme III. (a) 64-QAM constellation. (b) signal points for class 2 data (the points in the rectangle have the same parity bits).

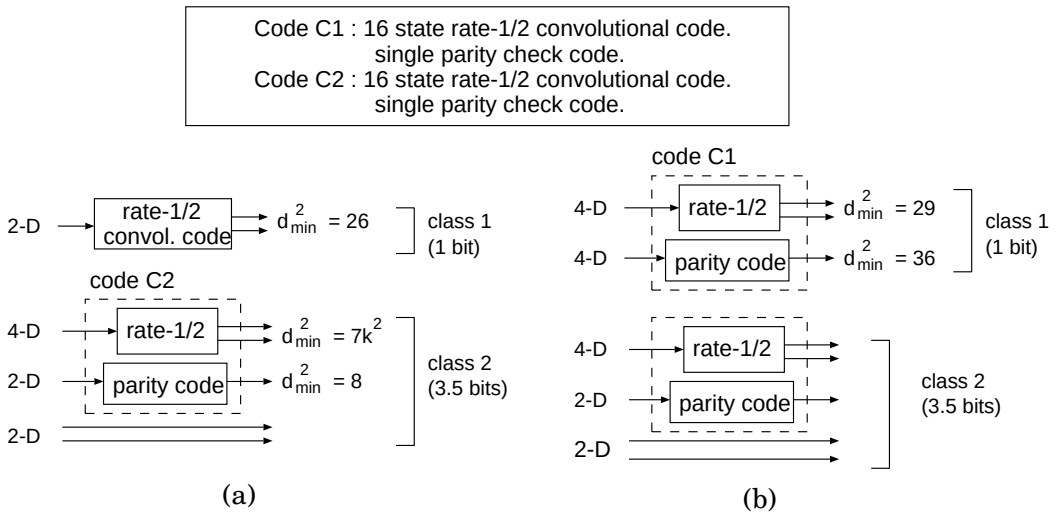

Figure 8: Code structures of scheme III (code C1 block is for class 1 data and code C2 block is for class 2 data). (a) Scheme III-A(2-D signalling). (b) Scheme III-B(4-D signalling).

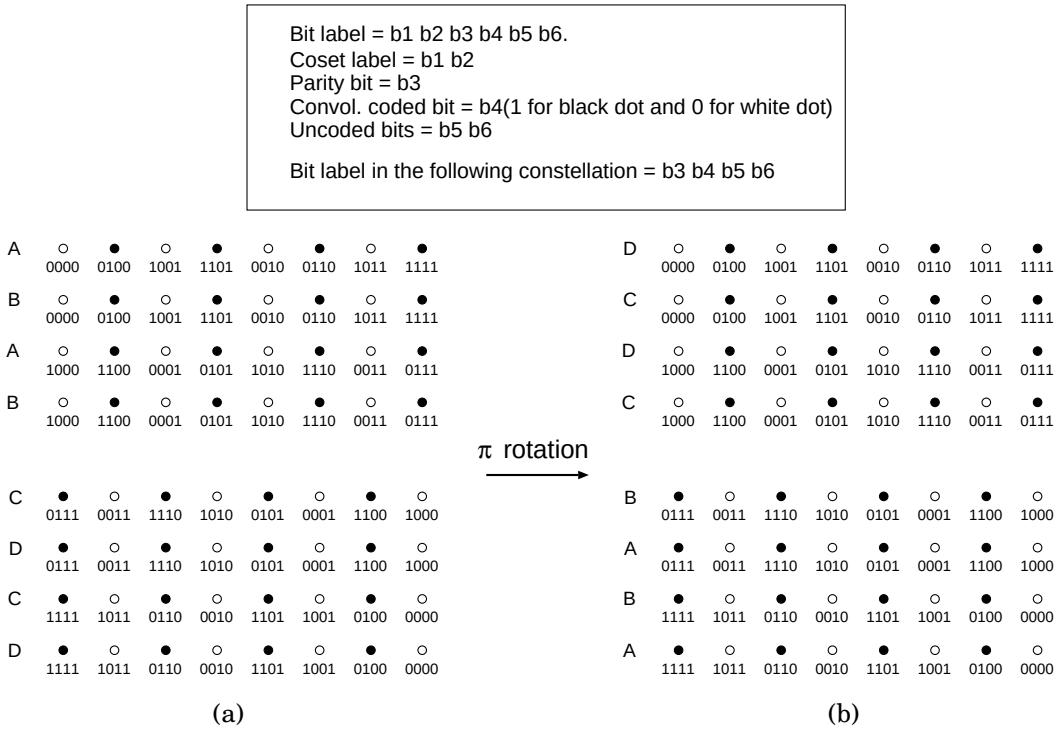

Figure 9: Signal constellation for 180^o RI scheme III. (a) Class 2 data bit allocation for 180^o RI code. (b) Received signal after 180^o phase error.

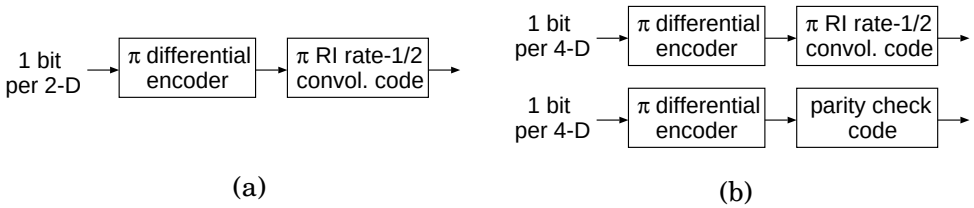

Figure 10: Structures of 180^o RI class 1 data protection code in scheme III. (a) 2-D signalling. (b) 4-D signalling.

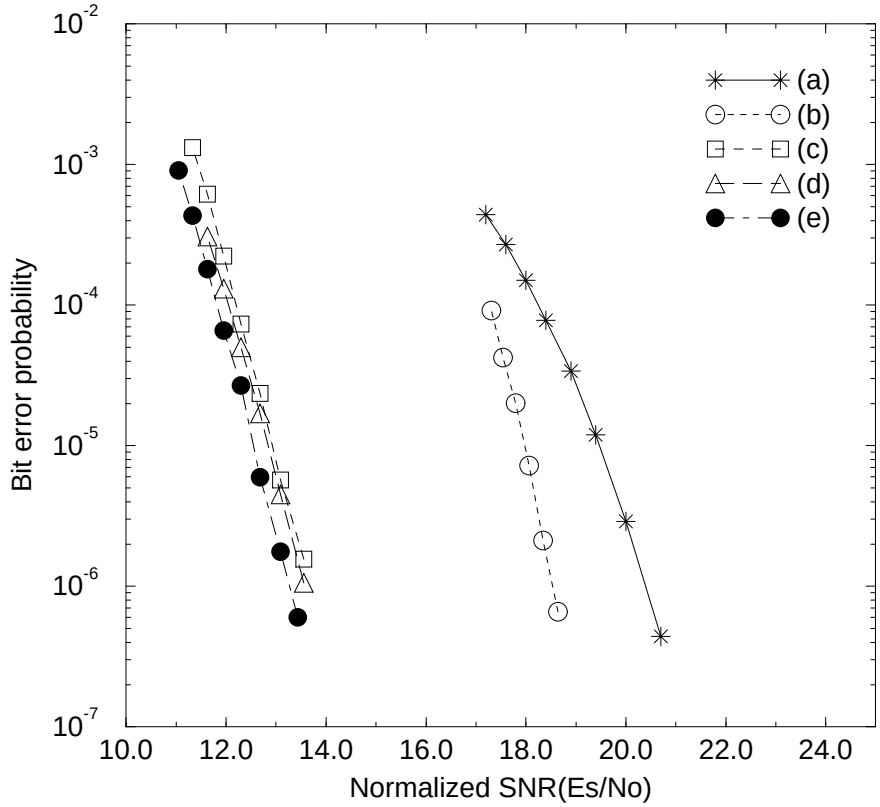

Figure 11: Simulation of scheme III in 4-D signalling(k^2 is 1.32) and 180^o RI 2-D and 4-D signalling. Block length L of parity check code is 20. (a) Uncoded 16-QAM. (b) Class 2 data protection code. (c) class 1 code (scheme III-A : 90^o RIC on 2-D signalling). (d) class 1 code (scheme III-B : 90^o RIC on 4-D signalling). (e) class 1 code (scheme III-B : non-RIC on 4-D signalling).